



3D design and numerical simulation of a check-valve micropump for lab-on-a-chip applications

J. Mazloun¹ · A. Shamsi¹

Received: 28 May 2020 / Revised: 18 August 2020 / Accepted: 28 September 2020 / Published online: 6 November 2020
© Springer-Verlag GmbH Germany, part of Springer Nature 2020

Abstract

In this paper, we concentrated on designing and simulation of check-valve micropump for on-chip applications. A series of simulations were carried out by using 3D two-way fully-coupled fluid structure interaction analysis in combination with Arbitrary Lagrangian-Eulerian (ALE) method to understand pumping chamber and inlet/outlet micro check-valves. After extraction of characteristic equations of each component, micropump main equation is solved to find time-domain pumping chamber pressure. Then, Effects of actuation amplitude and frequency on micropump's flow rate were studied for different chamber sizes from 2 mm to 4 mm. In addition, the effect of backpressure on micropumps' flow rate was evaluated. Using this method of simulation helps the researchers to estimate performance of micropump before initiating fabrication process.

Keywords Check-valve micropump · Membrane-type micro check-valve · Finite element analysis · Fluid-structure interaction · Volume displacement · MEMS and microfluidics-modeling

1 Introduction

In Recent decades, many researchers have tried to present fabrication methods for small micropumps capable of pumping extremely low volume of liquid. These efforts have resulted in implementation of several types of micropumps for applications in medicine, drug delivery, chemical and etc. [1–3]. Different available approaches in literature to develop micropumps are including diaphragm micropumps [4], Electrokinetics [5, 6], Magnetohydrodynamic micropumps [7] or surface acoustic wave micropumps [8]. Diaphragm (or mechanical) micropumps are categorized into valveless micropumps and Check-valve micropumps. Valveless micropumps generally have a nozzle diffuser structure at inlet and outlet of micropump; This type of micropumps is fabricated easily but it is susceptible to the leakage when backpressure increases [9, 10]. Check-valve micropumps,

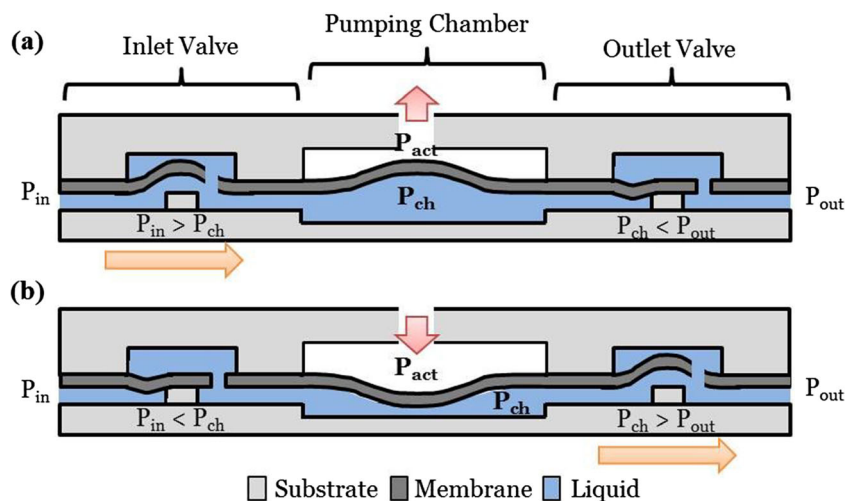
which are the focus of this work, opposed to valveless micropumps, have microvalves at their inlets and outlets which prevent backflow resulted from backpressure. Furthermore they have a more linear response and demonstrate overall better performance [4, 11–13]. As a result, check-valve micropumps are more popular in microfluidic systems [3]. The performance measures of micropumps include actuation voltage (or pressure), power consumption, operating frequency, flow rate, backpressure, pumping volume, pumping pressure, fabrication method, costs, dimensions, and finally capability of integration on the chips [2]. Figure 1 shows the structure of a diaphragm check-valve micropump that consists of one microvalve at inlet, one microvalve at outlet and one pumping chamber. Pumping chamber can be actuated using compressed inert gas, electrical field [14], electromagnetic field [15], piezoelectric force [4, 11, 12] and etc. Moreover, various types of active and passive microvalves such as membrane-type, cantilever-type, rotary-type, etc. can be used instead of the check-valves shown of Fig. 1 [16]. The membrane-based microvalve shown in Fig. 1 are one of the passive type in which whenever the inlet pressure exceeds the outlet pressure, the membrane is pulled upward and the microvalve opens, letting the fluid flow from inlet to the outlet. Conversely, whenever the outlet pressure is higher than the inlet pressure, the membrane moves downward to the valve-seat, closing the valve.

✉ J. Mazloun
jalil.mazloun@ssau.ac.ir

A. Shamsi
alireza.shamsi@ssau.ac.ir

¹ Department of Electrical Engineering, Shahid Sattari Aeronautical University of Science and Technology, Tehran, Iran

Fig. 1 Operating principles of micropump; **a** Suction operation phase or charge stroke causes the inlet valve to open while the outlet valve is closed, **b** Pumping operation phase or discharge stroke causes the outlet valve to open while the inlet valve is closed



The micropump shown in Fig. 1 has two operating phases known as charge phase and discharge phase. In the charge phase, the membrane on the pumping upper chamber is pulled up due to a negative pressure and induces a negative pressure at the lower pumping chamber of the pump. This negative pressure causes the inlet microvalve to open and the outlet microvalve to close, leading to the suction of liquid from inlet to the pumping chamber. In the discharge phase, the opposite of the aforementioned procedure occurs; in other words, a positive pressure acts on the membrane of the pumping chamber through the actuation port, pushing the membrane down and applying a positive pressure to the lower pumping chamber. This positive pressure causes the inlet valve to close and the outlet valve to open, leading to the pumping of the liquid out of pumping chamber to the outlet.

Most research works on check-valve micropumps, have focused on different fabrication methods, actuation mechanism, and valve designs and fewer works have paid attention to the simulation of this kind of micropumps [12, 17–19]. Even these few works that simulate check-valve micropumps, have modeled only some parts of the structure of the micropump, e.g. membrane, or a simplified microvalve. Moreover, among the performance measures of the micropump, no work has considered pumping pressure or pumping volume. It is noteworthy that actuation pressure differs from pumping pressure and one can become smaller or larger than the other [4, 13]. Both of the above mentioned shortcomings, along with other challenges in the check-valve micropump simulation will be addressed in this work. It goes without saying that simulation of valve-less micropumps is abundant in the literature due to structural simplicity.

In the past few years, finite element simulations have emerged as a powerful tool for predicting the microfluidic components behavior. This becomes much more vital when analyzing complex microfluidic systems. Zengerle et al. [13]

showed that a micropump can be modeled using electrical and fluidic systems. Bourouina et al. [20] verified this model for medical applications. During these years, many diaphragm micropumps have been manufactured, each trying to overcome certain deficiencies with varying degrees of success. In [21] for instance, non-linearity of the pump membrane are simulated using finite element method, and the micropump itself is simulated through modeling of diaphragm micropump component with their equivalent electrical components. Two main shortcomings of this work are the use of central deflection of membrane and the use of fully linear microvalve models. The former is addressed by Kang et al. [4], who has used the average deflection of the membrane and considered a rectangular membrane model which is common on MEMS devices, yet the latter is not addressed. Also, he didn't study Fluid-structure interaction of the pumping chamber and valves interactions. In [22], by means of two dimension fluid-structure interaction analysis which leads to simplifications, the size of inlet/outlet microvalves were optimized for diaphragm micropumps. These microvalves which were the sole focus of this work have been out of plane cantilever type, whereas in-plane cantilever valves were considered in [15]. In 2017, based on Bourouina's electrical model in [20], Fournier et al. designed a diaphragm micropump with cantilever microvalves for drug delivery applications, but its complex fabrication procedure results in a huge number of equivalent electrical components for simulation [23]. The actuation type used in this study was piezoelectric effect which is actuated by a square wave actuation voltage. Recently, Yazdi et al. [11], presented a piezoelectric check-valve micropump which had a circular pumping chamber and two circular diaphragm orthoplanar microvalves which was simulated using three dimensional fluid-structure analysis however their simulation method is limited only for a single type and shape of microvalves and can be extended to other types of microvalves or microvalves e.g. rectangular shapes.

In this paper, we shall address these problems and further develop the existing simulation methodology for mechanical micropumps by introducing several novelties. First, we simulate a mechanical micropump with a membrane-type check-valve, a venture missing from the available works. However, as mentioned before, membrane-type check-valve micropumps have been fabricated using various techniques. Our next contribution is in-depth characterization of membrane-type valves and pumping chamber by means of three dimensional fluid-structure interactions, whereas simplified two dimensional models prevail throughout the literature. The third novelty of this work is the exact modeling of non-linearity of membrane type microvalves by means of 6th order polynomial curve fitting approach that based on authors knowledge, never done before. This method enables us to accurately analyze any check-valve micropump via true modeling of fluid-structure interaction in three dimensions. It is important to mention that, in this work, we do not aim at optimization of distance of pumping chamber and valves from each other, nor do we try to study the stress and strain of the membrane of the valves or pumping chamber, or actuation equations of piezoelectric, electrostatic, electromagnetic actuation and their effects on the pump membrane. However, we will change pumping chamber size to study its effect on different micropump’s parameters.

The rest of this paper is organized as follows: in section 2 the proposed structure and material properties of the micropump, in addition to proposed fabrication process are discussed along with simulation procedure and the methods for extracting microvalve and pumping chamber characterizations equations. Section 3 presents the extracted characteristic equations, simulation results associated with the microvalves, pumping chamber and micropump, and discusses the entailing information. Finally, in section 4 the results of this paper will be compared with those existing in the literature to better understand advantages and disadvantages of each.

2 Material and methods

2.1 Basic principle and design

Figure 2 shows isometric, top and side views of the designed check-valve micropump used in this study. The designed micropump consists of three components: two membrane-type micro check-valves at inlet and outlet of the micropump, and one micropump’s main chamber. According to Fig. 2a, this micropump is actuated pneumatically via actuation port. This actuation can produce negative and positive pressure on the micropump’s membrane which results production of charge and discharge phases. Microvalves have the same size as indicated in Fig. 2b and c. The dimension of the valves and chamber can affect micropumps performance. The lower and

upper pumping chamber have diameter of D and height of h , which we will use them to design the pump with desire flow rate. Water was considered as aqueous solution with density of 1000 kg/m^3 and viscosity of 0.001 Pa.s . The membrane for valves and pumping chamber has thickness of $25 \text{ }\mu\text{m}$ with modulus of elasticity equal to 20 MPa , Poisson’s ratio of 0.49 and density of 1100 kg/m^3 [24] and the bulk of micropump was considered as impenetrable rigid body.

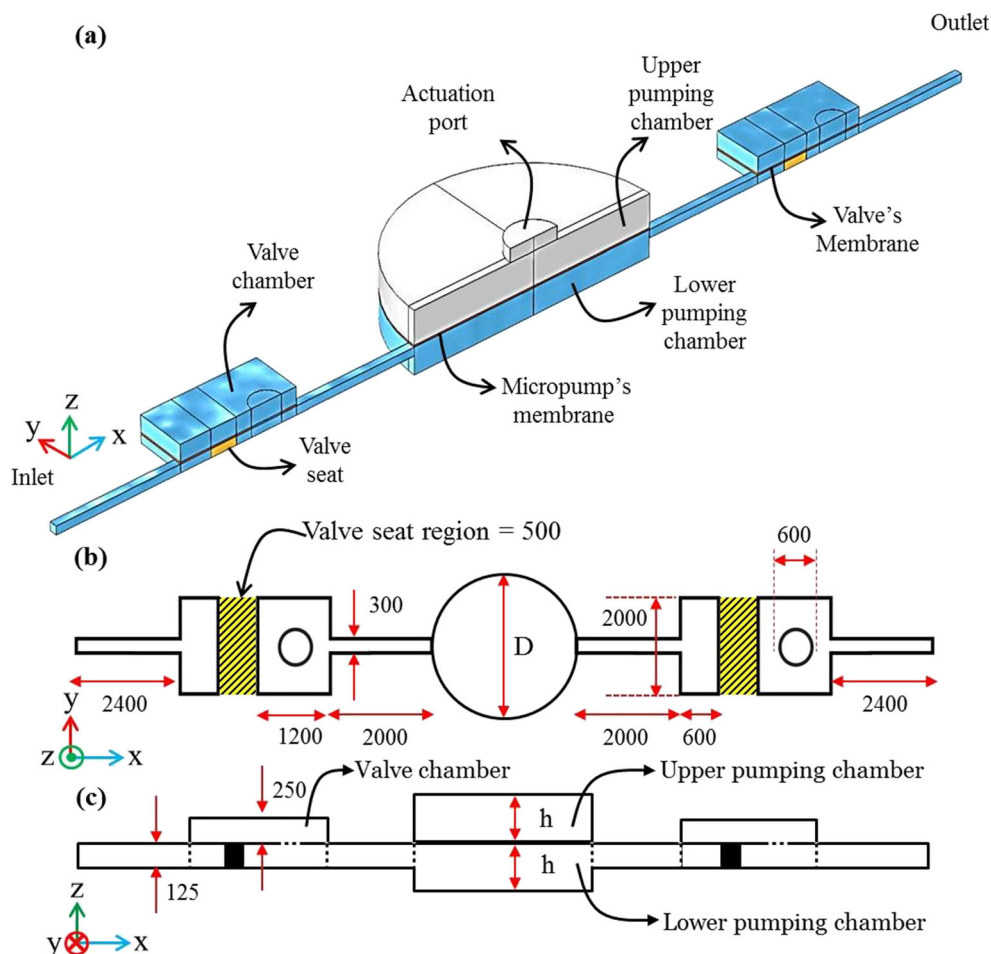
2.2 Modeling and simulation method

Due to complex fluid structure interaction between pumping chamber and inlet/outlet valves operation in micro-scale domain, the pressure inside the main chamber of the pump is not equal to the actuation pressure [10, 13]. The best approach for finding micropump performance is to conduct a 3-dimensional fully-coupled two-way fluid structure analysis. But, time-domain simulation of all components in a single finite element simulation will result in very high number of degree of freedom that needs high memory. In addition, this causes extremely long simulation which is practically impossible because of limited hardware resources, time and cost. As an example, Lai et al. [25] concentrated only on transient performance of a check valve at the opening period. Moreover, use of simplified simulation methods such as what Gong et al. [21] and has presented is not applicable to our micropump because of high nonlinear response of microvalves. To model and design CVP we mainly inspired from [13] to be able to determine time-domain pressure distribution in the lower pumping chamber. Afterwards, we can evaluate the pumping flow rate, estimate effect of actuation frequency, actuation pressure and backpressure on the performance of micropump. Differential equations describing behavior of the dynamics of the pump evaluated by continuity (conservation of mass) equation of the Navier-Stokes equations [26] which results to Eq. 1 [13]:

$$\frac{dP_{ch}}{dt} = \frac{Q_{iv}(p_{iv}) - Q_{ov}(p_{ov}) - \left. \frac{\partial V_m}{\partial P_{act}} \right|_{P_{ch}} \frac{dP_{act}}{dt}}{\left. \frac{\partial V_m}{\partial P_{ch}} \right|_{P_{act}} - \frac{dV_{iv}}{dP_{ch}} + \frac{dV_{ov}}{dP_{ch}} + \frac{dV_0}{dP_{ch}}} \tag{1}$$

Where, Q_{in} and Q_{out} are respectively the flow rate of inlet and outlet valve as a function of pressure difference across them, P_{act} is actuation pressure and P_{ch} is pressure inside the chamber. In our simulation, we will exert a simple pneumatic pressure as P_{act} however; it is rather easy to actuate the pump using electrostatic, electromagnetic or piezoelectric energy and convert their energy to the force per unit area. Finally, V_m , V_0 , V_{iv} and V_{ov} are volume displacement of the pumping chamber’s membrane, total micropump’s chamber volume, inlet and outlet microvalves volume displacement, respectively. This equation expresses that we can simulate microvalves

Fig. 2 Structure and schematic design of the micropump; **a** isometric view, **b** top view, **c** side view - all dimensions are in micrometer



and pumping chamber separately and by substitution of their characteristic equations inside Eq. 1 the pressure inside lower pumping chamber can be calculated. However, due to complexity of this equation, it is inevitable to use numerical methods to solve this equation.

In a detailed explanation, at the first step we will simulate microvalves and pumping chamber in the next sections of current paper using fully-coupled two-way fluid structure interaction analysis. Differential equations describing behavior of the fluid domain are well-known Navier-Stokes equations [26] while the calculations for the structural domain are based on the impulse conservation equation [27]. These equations coupled into each other using two-way fluid-structure interaction analysis [27]. To do so, all the simulations have been done using general finite element software (such as Adina, Ansys, Comsol, ...) which is available on markets. Among them Comsol Multiphysics was used for this study. Then, we shall extract volume displacement and flow rate equations of microvalves and pumping chamber to substitute the extracted equations in the Eq. 1. The relative equations of volume displacement and flow rate will be achieved by using 6th order polynomial curve fitting. To do so, general mathematical software (such as Matlab student version, Wolfram Mathematica,

MS Excel, ...) is tailored to our needs. Afterwards, we will use numerical simulation once more to evaluate lower pumping chamber pressure by solving Eq.1. In the fourth (and last) step, this calculated pressure will be exerted on the microvalves equations to find the pumping flow rate and study the effect of actuation frequency and amplitude on the micropump. It is necessary to say that to solve Eq.1 we must change the units into standard scales otherwise the solver will either generate wrong or diverged results. In other words, instead of $\mu\text{L}/\text{min}$ for flow rate we shall use m^3/s . At last, we should mention that all the simulations were implemented on 64-bit Windows 7 platform while hardware configuration used for simulation is combination of 16 core Intel® CPU with 24 GB of RAM.

2.3 Simulation method of the microvalve

Figure 1 and Fig. 2 shows the design and dimensions of the inlet/outlet micro check-valves. This membrane-type microvalve has two operation modes known as forward mode and reverse mode. When pressure at valve inlet is higher than valve's outlet, the membrane goes upward letting the fluid pass through the valve which is called forward mode

operation. In reverse mode operation, valve’s outlet pressure is higher than inlet, forcing the membrane toward valve-seat and closes the valve. Two main characteristics of microvalves for designing of diaphragm micropump are volume displacement (that we denoted them as V_{iv} and V_{ov}) and flow rate (that we denoted them as Q_{iv} and Q_{ov}). Because of very non-linear behavior of the microvalves in forward-mode operation, this information extracted from two-way fully-coupled FSI analysis in order to describe the valves operation in formulation of the pump. However, due to the laminar nature of microfluidic systems, we used incompressible laminar formulation for fluid domain. Also, geometry nonlinearity was considered for structural analyzer of the FSI solver. Therefore, non-linear deformation of the membrane, capacitive and resistive effects of valve and its related microchannels were completely considered [28] because three dimensional fully-coupled fluid-structure interaction analyses was performed. The initial condition and boundary condition for simulation of microvalve are including: (1) Initial condition for all variables was zero, (2) No-slip and no-penetration boundary condition was considered for all solid walls, (3) at forward mode operation, the fluid was driven by pressure at inlet which was swept from 0 to 3 kPa, (4) at reverse-mode operation, the pressure at outlet was swept from 0 to 7 kPa, (5) To reduce number of elements and computation time symmetry boundary condition along x-axis was used, (6) we used Arbitrary Lagrangian-Eulerian (ALE) algorithm to allow the mesh move freely because of movement of solid membrane inside the fluid domain [29, 30]. A combination of structured and unstructured mesh was used to discretize designed check-valve model with over 850,000 DOF. The relative equations of valve volume displacement (with unit of m^3) and flow rate (with unit of m^3/s) will be extracted using 6th order polynomial curve fitting that will be presented in the results and discussion section.

2.4 Simulation method of the pumping chamber

The design of the pumping chamber was shown in Fig. 2. Due to the fact that the deflection of the chamber’s membrane is larger than the membrane thickness, and at the same time chamber’s radius is much larger than membrane thickness, we have to use nonlinear formulation to calculate and simulate membrane displacement and resulted volume displacement. Maximum non-linear displacement of circular membrane and its relative volume displacement can be calculated using [31, 32]:

$$\delta = t_h \left(\frac{3 R^4}{16 E t_h^4} \right)^{1/3} P^{1/3} \tag{2}$$

$$V_m = \frac{\pi \delta}{6} (3 R^2 + \delta^2) \tag{3}$$

Where, t_h is membrane thickness, R is chamber’s radius, δ and V_m are non-linear displacement and volume displacement of the membrane, respectively. At simulation level, we used three dimensional FSI analyses using more than 630,000 DOF to simulate chamber’s behavior. Other details including: (1) ALE algorithm was used to have mesh motion due to movement of solid membrane inside the fluid domain. (2) We simulated three pumping chambers with diameters (D) of 2, 3 and 4 mm. Height of each chamber can be calculated easily from Eq. 2. (3) The actuation pressure exerted on the membrane of micropump was swept from 0 to 3 kPa. Since the membrane has isotropic material properties, simulation of one of charge or discharge phase will give us the appropriate results. (4) Initial and other boundary conditions are similar to microvalves simulation. It is necessary to say that since the effect of microchannels between pumping chamber and inlet/outlet microvalves was considered in the simulation of microvalves (in the previous subsection of the paper), it does not need to simulate the both sides microchannels in the simulation of the pumping chamber.

2.5 Proposed fabrication process

Albeit we have concentrated on numerical simulation so far, to show the feasibility of our design in practice, here is a proposed fabrication process to implement the CVP. Since use of thermoplastic material was suggested by several researchers [33, 34] we also used its material properties in our study and we now suggest an easy fabrication process to be able to make the CVP. The following steps propose the fabrication process, and Fig. 3 visualizes these steps. According to [35–37], we propose use of Poly-methyl meth-acrylate (PMMA) as substrate. First, the design of each layer is drawn in AutoCAD® and is sent to micromilling machine interface software to transfer the pattern to the substrate (Fig. 3a). Then, by appropriate setting of micromilling machine we can engrave microchannels and valve/pumping chambers according to the designed width and depth. Inlet/outlet holes can be made at this step (Fig. 3b). After micromilling process of the substrates there need a surface treatment to reduce roughness of the microchannels and chambers [35, 38]. Use of solvent vapor is suggested [39] for this aim. Afterwards, thermoplastic elastic membrane is cut in appropriate size using a utility knife blade. At last, layers can be aligned appropriately and can be thermally bonded based on the previously reported process (Fig. 3c) [19].

3 Results and discussion

In this Section, we will check results of microvalve’s FSI analysis for its both operation modes. Then, pumping chamber’s FSI analysis will be studied. In the third step, volume

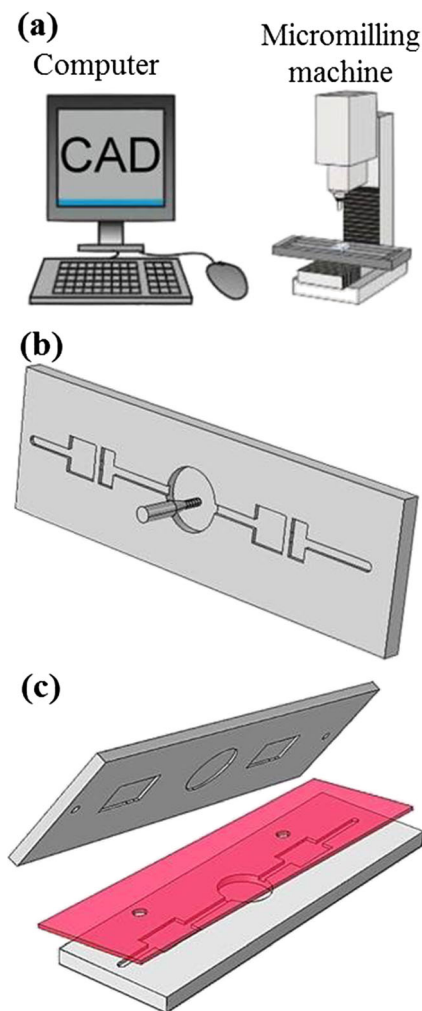


Fig. 3 Proposed fabrication process

displacement and flow rate of microvalves and pumping chamber will be evaluated (with standard unit scales) to be extracted as equation. We will use these extracted characteristic equations to solve Eq. 1 and find out pumping chamber pressure. From that, we can reach to the micropump's characteristic performance that will be explained in subsection 3.4 through the end.

3.1 Results of microvalve simulation

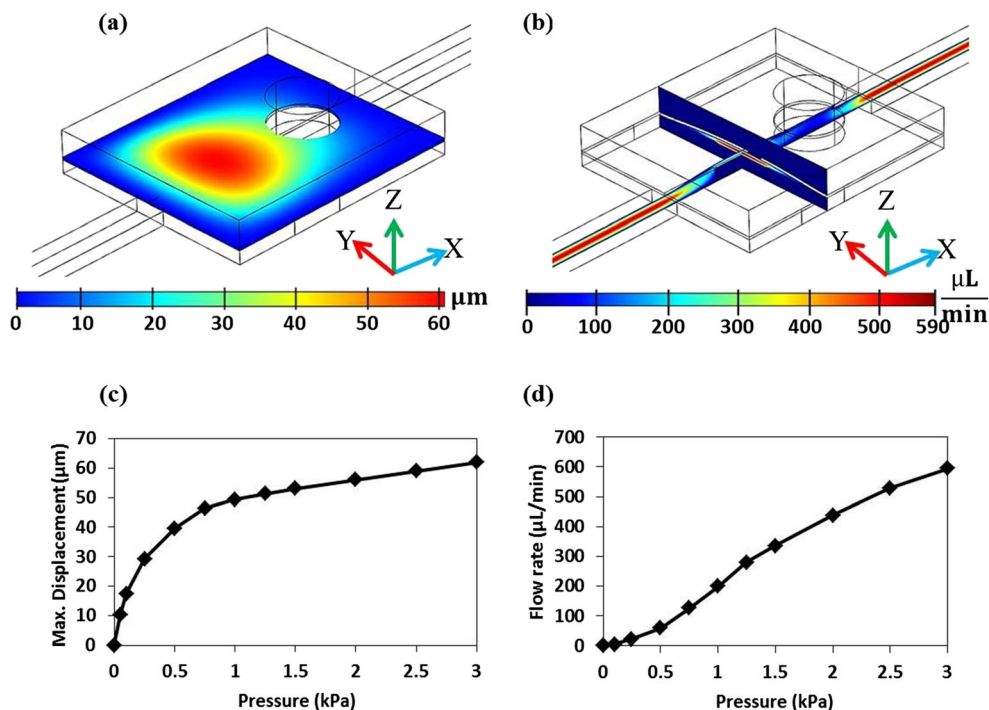
We first analyzed reverse mode operation of the microvalve by exerting a maximum pressure of 7 kPa at the valve's outlet whilst its inlet was kept at zero. This was to measure its reverse mode leakage rate that

resulted in 7.5 nL/min which is extremely low. This shows the valve can perfectly block flows in reverse mode for this reason we can neglect back flows. Afterward, by swapping the inlet/outlet pressure, a positive pressure was exerted on the inlet to measure microvalve's forward mode flow rate and membrane's displacement. Figure 4a and b show isometric view of displacement of valve's membrane and its flow rate while its inlet actuated using 3 kPa pressure. When the valve's inlet pressure increases from 0 to 3 kPa, membrane's maximum displacement grows approximately to 65 μm (Fig. 4c) which is far away from ceiling of the valve (that has 250 μm height) and liquid passes the valve with rate of about 600 $\mu\text{L}/\text{min}$. Figure 4d plots microvalves flow rate versus forward mode inlet pressure. This plot shows that the micro check-valve can operate analogous to an electronic diode. At last we should mention that to have an overview to the natural frequencies of microvalve's solid membrane, we also carried out a modal analysis. Membrane's first measured natural frequency was about 1423 Hz which was in the same direction of z-axis (Fig. 4a). This might be important when micropump is actuated at higher frequencies that we will discuss this issue in the next subsections.

3.2 Results of pumping chamber simulation

Surface plot of maximum chamber displacement with diameter of 4 mm while actuation pressure was 3 kPa, was shown in Fig. 5a. To evaluate pumping chamber performance and capability, different chamber's diameter was used for FSI simulation. We simulated charge (suction) phase operation of micropump however due to linear and isotropic material properties of the membrane, the discharge phase has the same absolute results but in opposite direction. Figure 5b shows maximum displacement of pumping chamber versus actuation pressure in which, 103.8, 182.3 and 269.3 μm was maximum displacement of 2, 3, and 4 mm diameter while actuation pressure was 3 kPa. According to Fig. 2c and Eq. 2, the height parameter (h) of upper/lower pumping chamber is now calculated which is approximately equal to maximum deflection of membrane under maximum pressure of 3 kPa. Eventually, to have an insight to the pumping chamber natural frequency, we also carried out a modal analysis for the solid membrane with different diameters. The resulted membrane's natural frequency with diameters of 2, 3 and 4 mm was 1902, 833.66 and 466.34 Hz.

Fig. 4 Fluid structural interaction analysis of the micro check-valve; **a** Contour view of inlet/outlet valve’s membrane displacement with 3 kPa of pressure at the valve’s inlet, **b** flow velocity of liquid in the valve with 3 kPa of pressure at the valve’s inlet, **c** Maximum displacement of the valve versus applied pressure, **d** flow rate passing through the valve versus applied



3.3 Extracted characteristics equations

As we explained before, we need to evaluate microvalve and pumping chamber characterization equations to be able to solve Eq. 1 and find out micropump’s chamber pressure. Figure 6a and b show volume displacement and flow rate of microvalves. Each black point is a result of FSI analysis. These plotted results were changed into standard scale to unify all unit scales in the micropump main Eq. 1. The equations for microvalve extracted from Fig. 6a and b using 6th order polynomial curve fitting is illustrated in Eqs. 4 and 5, respectively. These curves were plotted as a red line in Fig. 6a and b, respectively.

$$\begin{aligned}
 Q_{in} = & -(1.890e-28)P^6 + (1.641e-24)P^5 - (4.895e-21)P^4 \\
 & + (4.935e-18)P^3 + (1.094e-15)P^2 \\
 & + (7.705e-13)P; R^2\text{-squared} \\
 = & 99.99
 \end{aligned}
 \tag{4}$$

$$\begin{aligned}
 V_{iv} = & -(5.806e-30)P^6 + (5.840e-26)P^5 - (2.296e-22)P^4 \\
 & + (4.471e-19)P^3 - (4.547e-16)P^2 \\
 & + (2.460e-13)P; R^2\text{-squared} \\
 = & 99.79
 \end{aligned}
 \tag{5}$$

The above equations are for outlet micro check-valve. In other words, they are valid for chamber pressures

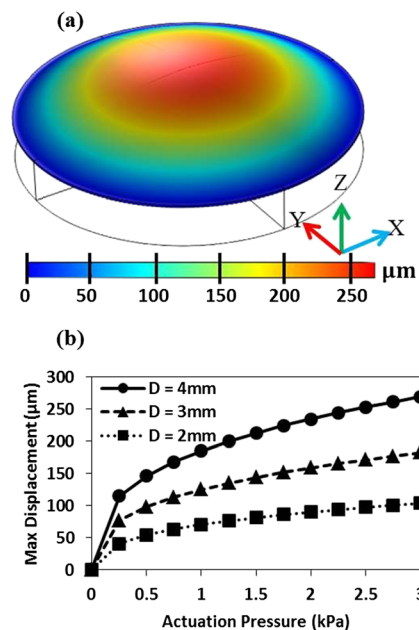


Fig. 5 Fluid structural interaction analysis of micropump’s deformation membrane; **a** Contour plot of membrane’s displacement with diameter of 4 mm and actuation pressure of 3 kPa, **b** Maximum displacement of membrane with different diameters as a function of actuation pressure

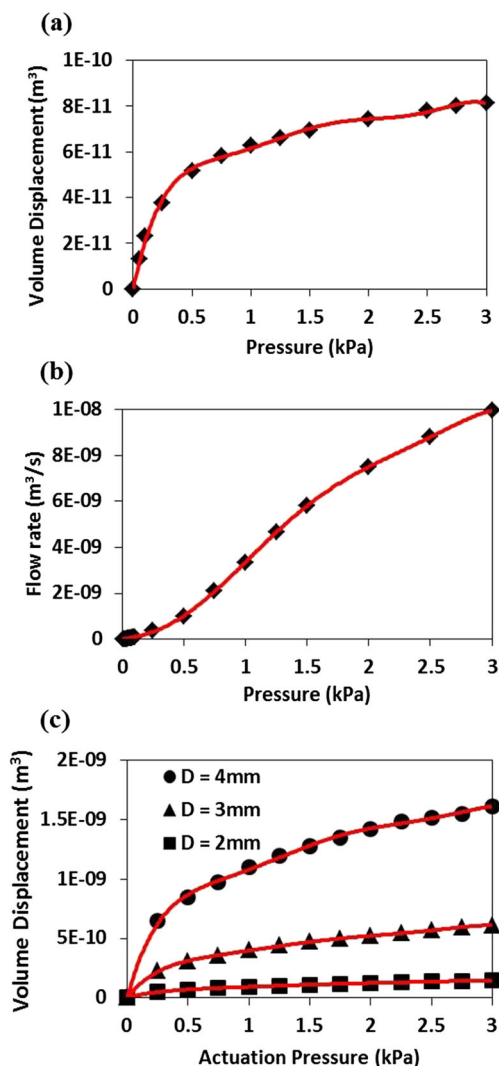


Fig. 6 Curve fitting plots; **a** Volume displacement of membrane-type micro check-valve vs pressure, **b** Flow rate of membrane-type micro check-valve vs pressure, **c** Volume displacement of pumping chamber with different diameters as a function of actuation pressure – the red lines are 6th order polynomial fitting curve in standard unit scale

higher than or equal to zero. As explained in previous sections, the microvalves have extremely low leakage rate. For this reason, the flow rate for pressures lower than zero was neglected for outlet microvalve. With little manipulation, inlet microvalve characterization equations can be easily extracted that must be valid for chamber pressure lower than or equal to zero while its leakage rate for pressures higher than zero is zero.

The same procedure has been done for volume displacement of pumping chamber with different diameters which was shown in Fig. 6c. The equation of volume displacement for pumping chamber with diameters of 2, 3 and 4 mm is illustrated in Eq. 7 through Eq. 8, respectively. These equations which extracted using 6th order polynomial curve fitting technique are:

$$\begin{aligned} V_{m|D=2\text{mm}} &= -(3.752\text{e-}30)P^6 \\ &+ (3.897\text{e-}26)P^5 - (1.599\text{e-}22)P^4 \\ &+ (3.311\text{e-}19)P^3 - (3.711\text{e-}16)P^2 \\ &+ (2.548\text{e-}13)P; R^2\text{-squared} \\ &= 99.95 \end{aligned} \quad (6)$$

$$\begin{aligned} V_{m|D=3\text{mm}} &= -(2.442\text{e-}29)P^6 \\ &+ (2.476\text{e-}25)P^5 - (9.874\text{e-}22)P^4 \\ &+ (1.971\text{e-}18)P^3 - (2.094\text{e-}15)P^2 \\ &+ (1.283\text{e-}12)P; R^2\text{-squared} \\ &= 99.93 \end{aligned} \quad (7)$$

$$\begin{aligned} V_{m|D=4\text{mm}} &= -(6.463\text{e-}29)P^6 \\ &+ (6.854\text{e-}25)P^5 - (2.846\text{e-}21)P^4 \\ &+ (5.850\text{e-}18)P^3 - (6.278\text{e-}15)P^2 \\ &+ (3.734\text{e-}12)P; R^2\text{-squared} \\ &= 99.89 \end{aligned} \quad (8)$$

The regression factor (R^2) of above equations shows the quality of matching between black points and the fitted red lines. All of these equations were substituted in the Eq. 1 and solved using time domain numerical solvers to reach lower pumping chamber pressure. These results are explained in the following subsections.

3.4 Time domain responses of the pump

After appropriate substitution of previous extracted equations into the Eq. 1 and solving it using FEM solvers, we first tried to evaluate micropump chamber pressure and flow rate. Figure 7 shows pressure and flow rate of the micropump as a function of time while actuation frequency is 5 Hz, chamber diameter of 3 mm and zero backpressure. The dashed line showed in Fig. 7a is actuation pressure and the bolded line is the pressure inside the pumping chamber. It is obvious that the pressure inside the pumping chamber (812 Pa) is less than actuation pressure (1000 Pa). Since we started the actuation process of the pumping from suction phase thus there is a negative pressure inside the chamber and this resulted the inlet valve to be open while the outlet valve is closed. In Fig. 7b, the operation of suction phase and pumping phase is observable, in which the inlet valve

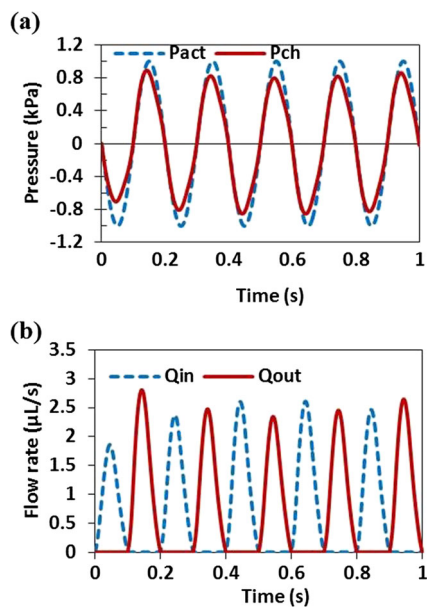


Fig. 7 Pressure and flow rate of the micropump as a function of time with actuation frequency is 5 Hz, chamber diameter of 3 mm and zero backpressure; **a** Plot of actuated pressure and resultant chamber pressure, **b** flow rate of micropump at charge stroke (Q_{in}) and discharge stroke (Q_{out})

(the blue dashed line) is only active in suction phase and outlet valve (the red bolded line) in only open in pumping phase. After several working periods the amplitude of valves flow rate become approximately equal.

3.5 Effect of actuation pressure

In this subsection, we tried to find out the effect of actuation pressure on functionality of the pump. Figure 8a shows the amount of liquid pumped by the designed pump with different chamber diameter in a 10 s time-frame. In this figure, actuation pressure and frequency were 1 kPa and 1 Hz, respectively. This result shows the chamber with diameter of 2, 3 and 4 mm can pump the amount of 5.25, 16.45 and 29.75 μL of liquid per minute. Figure 8b and c demonstrate the pressure inside the pumping chamber and flow rate versus actuation pressure while actuation frequency is kept at 1 Hz. It is tangible that the pressure inside the pumping chamber is always smaller than the actuation pressure and this relation is almost linear however if we increase the actuation pressure this relation will become nonlinear. When the diameter of pumping chamber is 2, 3 and 4 mm and actuation pressure is equal to 2 kPa, the maximum pressure inside the pumping chamber will be 447, 1037 and 1408 Pa, respectively.

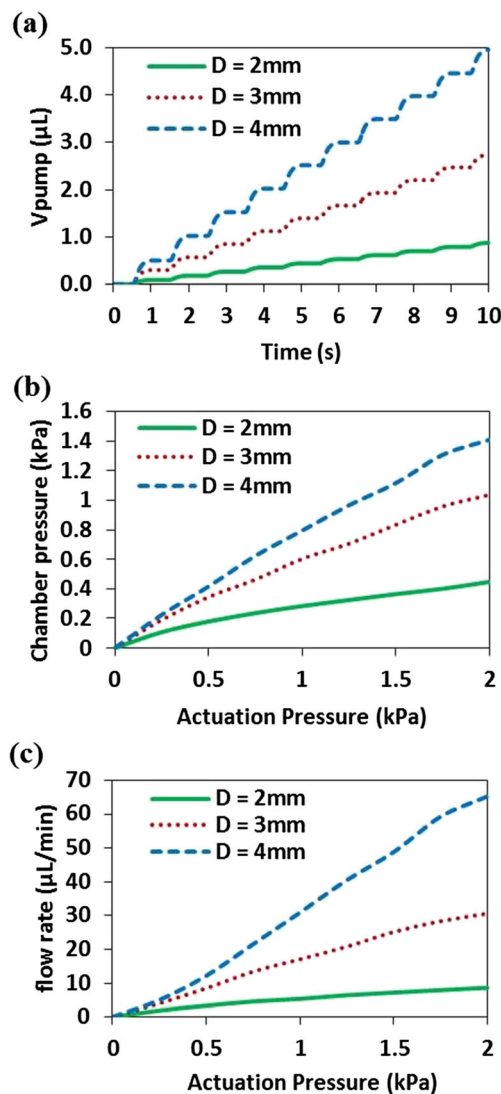


Fig. 8 **a** Volume pumped versus time, actuation pressure and frequency are 1 kPa and 1 Hz, respectively, **b** Chamber pressure versus actuation pressure while actuation pressure is kept at 1 Hz, **c** Valve flow rate versus actuation pressure while actuation frequency is kept at 1 Hz

3.6 Effect of actuation frequency

We guess the increase of actuation frequency can increase the pumping flow rate. To evaluate this assumption we ran several simulations for each pumping chamber diameter. According to Fig. 9, increase of actuation frequency increases pumping flow rate and after a certain frequency, which is about 5 Hz in our model, it gradually decreases. For example, for chamber diameter of 3 mm, increment of frequency from 1 to 3 and then 5 Hz, increases the flow rate from 16.4 to 23.3 and then 24.8 $\mu\text{L}/\text{min}$. These values for chamber diameter of 4 mm, increases from 29.3 to 39.2 and then 39.9 $\mu\text{L}/\text{min}$. One of the concerns in simulation of check valve

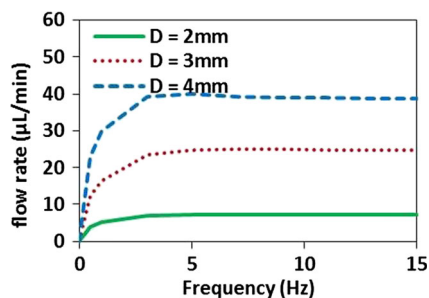


Fig. 9 Micropump flow rate as a function of actuation frequency for different chamber diameters while zero backpressure was considered for the pump. Actuation amplitude in this study is 1 kPa

micropump is the delay between actuation pressure on the membrane and the reflection displacement of membrane to that pressure. As mentioned before, from modal analysis of pumping chamber's solid membrane and microvalves, the lowest natural frequency was above 450 Hz. Thus, because the frequency of actuation pressure (maximally 10 Hz) is far away from natural frequencies of valves and pumping chamber, this delay can be ignored without any concern. Also, we didn't observe any delay between actuation pressure and valve/pump's time-domain response. However, for higher actuation frequencies this can produce some side effects on the operation of the micropump which must be considered.

3.7 Effect of backpressure

The effect of back pressure was not considered so far. Here, we modified the extracted equations and imported effect of back pressure into the Eq. 1 to study its effect on pumping flow rate. Figure 10a demonstrates the volume of liquid pumped using 1 kPa of actuation pressure and 1 Hz of actuation frequency on chamber size of 4 mm. Increase of back pressure from 0 to 400 and then 800 Pa decreases the flow rate from 28.4 to 16 and finally 3.68 $\mu\text{L}/\text{min}$. Higher actuation frequency can have better response while back pressure is not as high as actuation pressure (Fig. 10b). It is observable from Fig. 10b that by increment of back pressure pumping flow rate decreases linearly and finally backpressure of approximately 950 Pa was able to reach the flow rate to zero. This is similar to what other researchers reported previously too [4, 12, 17, 40]. Figure 10c shows pumping flow rate versus backpressure with different chamber size. In this analysis, actuation pressure and frequency were 1 kPa and 1 Hz, respectively. Similar to Fig. 9b, flow rate decreases linearly with respect to increment of backpressure and zero backpressure was again 950 Pa, albeit the larger chamber size could produce larger flow rate at lower backpressure.

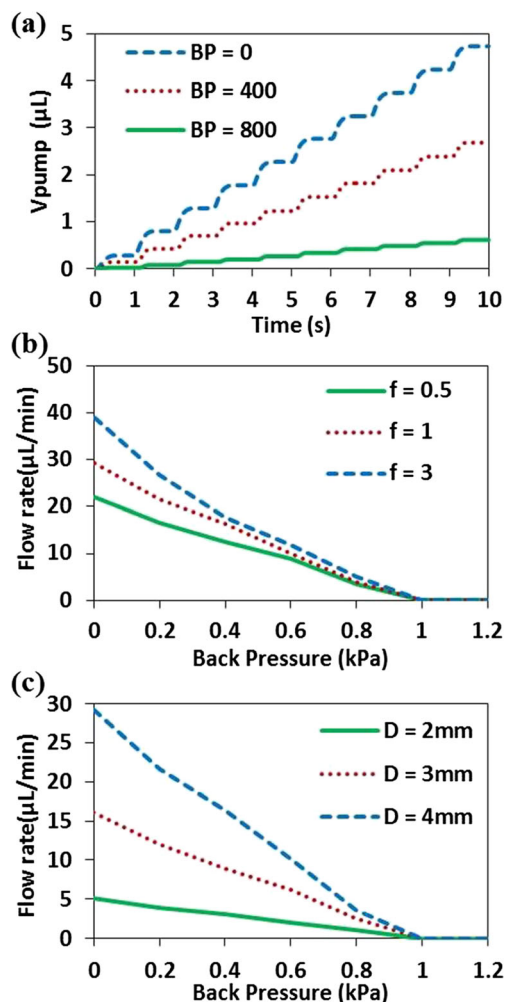


Fig. 10 Effect of backpressure on micropump operation; **a** pumped volume in time domain for different backpressure while chamber diameter is 4 mm, **b** flow rate versus backpressure at different actuation frequency while chamber diameter is 4 mm, **c** flow rate versus backpressure for different chamber diameters while actuation frequency is 1 Hz

3.8 Comparison

In the following, we compared advantageous and disadvantageous of current micropump with other reported micropumps. Ref [18] fabricated a pneumatically actuated micropump on PDMS substrate. This micropump had 4 mm of chamber diameter and used two in-plane cantilever microvalves.

The channels' depth and width were $100 \times 350 \mu\text{m}^2$. This micropump with actuation pressure and frequency of 10 kPa and 3 Hz has the ability to pump 200 $\mu\text{L}/\text{min}$. Its flow rate plot is very similar to Fig. 9. In addition, it could pump fluid up to 6 kPa of backpressure. Its response to backpressure is very similar to Fig. 10. The main drawback of this micropump is its microvalves leak flow in reverse mode of operation which reduces efficiency of the micropump.

Table 1 A comparison of the current micropump with some previously fabricated devices

		Frequency		Chamber	Chamber	Q	Backpressure	Vpump
Ref.	Act.Method	(Hz)	Actuation	size (mm)	shape	($\mu\text{L}/\text{min}$)	(kPa)	(μL)
This work1	Compressed air	1	1(kPa)	2	Circular	5.25	0.95	0.09
This work2	Compressed air	1	1(kPa)	3	Circular	16.45	0.95	0.27
This work3	Compressed air	1	1(kPa)	4	Circular	29.75	0.95	0.5
[18]	Compressed air	3	10(kPa)	4	Circular	200	6	3
[41]	Compressed air	26	68.9(kPa)	7.×2.5	Rectangular	488	–	–
[42]	Piezoelectric	3	100(v)	–	–	41.6	–	0.2
[11]	Piezoelectric	10	60(v)	1.5	Circular	1.62	6.8	–

These results, which is a fabricated micropump is very similar to our simulated micropump which verifies the accuracy of our work.

The proposed mechanical micropump reported by Bui et al. [41], is comprised of a rectangular chamber with size of $2.5 \times 7.5 \text{ mm}^2$ and two active check valves that was fabricated on PDMS. This micropump was actuated pneumatically using 26 Hz and 68.9 kPa of actuation frequency and pressure, respectively, that could produce flow rate of 488 $\mu\text{L}/\text{min}$. Unfortunately, the authors didn't provide any information on backpressure. They concentrated on development of a numerical method for design of rectangular pumping chamber with active check valves. In our work however, we considered a smaller chamber size and actuation pressure while according to Figs. 6 through 10 it has better performance.

Fillon et al. [42] developed a piezoelectric actuated micropump for drug delivery. This micropump with actuation frequency and voltage of 3 Hz and 100 V was able to produce 41.6 $\mu\text{L}/\text{min}$ of flow rate and 0.2 μL of fluid volume stroke. The details of size and shape of pumping chamber and microvalves are not reported in this work. In our work, we have higher fluid stroke volume and flow rate which result of chamber size and elastic membrane's material properties.

Recently, Yazdi et al. [11] developed a new numerical method for piezoelectric micropump for drug delivery and cooling system applications. The maximum predicted outflow was 1.62 $\mu\text{L}/\text{min}$, obtained at 10 Hz of working frequency and 60 v of input voltage. After geometrical optimization the outflow was increased to 25 $\mu\text{L}/\text{min}$. That circular pumping chamber had 1500 μm of diameter and two circular inlet/outlet check valves with diameter of 180 and 500 μm , respectively. The numerical simulation method presented by [11] is only applicable to circular-shaped pumping chamber and check valves. However, the numerical method of our work can be exerted on

micropumps with any geometry and sizes of pumping chamber and check valves.

In the end, it is evident that by comparing the results of this paper with the existing literature (Table 1), one can confirm the consistency of the numerical results and figures provided in this work. Moreover, the proposed simulation methodology facilitates the researchers in predicting the micropump behavior and characteristics in full detail before initiating fabrication.

4 Conclusion

In this paper, inspired by Zengerle [13], we proposed a novel numerical analysis for a check-valve micropump. To do so, we first implemented a micropump using two membrane-type micro check-valves. Then, we employed a three dimensional fully-coupled FSI analysis to simulate the pumping chamber and inlet/outlet microvalves. This is opposed to the prevailing trends where 2D simplified models are generally used due to hardware and software limitations. Next, we used a 6th order polynomial curve fitting method to model the exact nonlinear response of the membrane-type micro check-valve and to extract the required characteristic equations for solving the micropump's main equation; an approach not taken before. Finally, we evaluated the time-domain pressure of the lower pumping chamber and used this pressure to better understand the effects of actuation pressure and frequency on the micropump behavior.

References

1. Au AK, Lai H, Utela BR, Folch A (2011) Microvalves and micropumps for BioMEMS. *Micromachines* 2(2):179–220

2. Wang Y-N, Fu L-M (2018) Micropumps and biomedical applications—a review. *Microelectron Eng* 195:121–138
3. Mohith S, Karanth PN, Kulkarni S (2019) Recent trends in mechanical micropumps and their applications: a review. *Mechatronics* 60:34–55
4. Kang J, Auner GW (2011) Simulation and verification of a piezoelectrically actuated diaphragm for check valve micropump design. *Sensors Actuators A Phys* 167(2):512–516
5. Mehdipour M, Vafaie RH, Pourmand A, Ghavifekr HB (2012) A new miniaturized traveling-wave electro-osmotic micro-pump by low velocity of fluid for lab-on-a-chip application," in 20th Iranian Conference on Electrical Engineering (ICEE2012), pp. 223–227: IEEE
6. Dehghan Manshadi MK, Khojasteh D, Mohammadi M, Kamali R (2016) Electroosmotic micropump for lab-on-a-chip biomedical applications. *International Journal of Numerical Modelling: Electronic Networks, Devices and Fields* 29(5):845–858
7. Derakhshan S, Yazdani K (2016) 3D analysis of magnetohydrodynamic (MHD) micropump performance using numerical method. *J Mech* 32(1):55–62
8. Rimsa R, Smith A, Wälti C, Wood C (2017) A planar surface acoustic wave micropump for closed-loop microfluidics. *Appl Phys Lett* 111(23):234102
9. Nhu CN, Van LL, Ngoc AN, Dau VT, Bui TT, Duc TC (2018) A valveless micropump based on additive fabrication technology. *Int J Nanotechnol* 15(11–12):1010–1023
10. Wang T et al. (2018) Numerical and experimental study of valveless micropump using dynamic multiphysics model," in 2018 IEEE 13th Annual International Conference on Nano/Micro Engineered and Molecular Systems (NEMS), pp. 300–303: IEEE
11. Farshchi Yazdi SAF, Corigliano A, Ardito R (2019) 3-D Design and Simulation of a Piezoelectric Micropump. *Micromachines* 10(4):259
12. Ma H-K, Hou B-R, Wu H, Lin C-Y, Gao J-J, Kou M-C (2008) Development and application of a diaphragm micro-pump with piezoelectric device. *Microsyst Technol* 14(7):1001–1007
13. Zengerle R, Richter M (1994) Simulation of microfluid systems. *J Micromech Microeng* 4(4):192
14. Corigliano A, Ardito R, Bertarelli E, Ferrera M (2018) Micropump with electrostatic actuation," ed: Google patents
15. Ni J, Wang B, Chang S, Lin Q (2014) An integrated planar magnetic micropump. *Microelectron Eng* 117:35–40
16. Oh KW, Ahn CH (2006) A review of microvalves. *J Micromech Microeng* 16(5):R13
17. Kang J, Mantese JV, Auner GW (2008) A self-priming, high performance, check valve diaphragm micropump made from SOI wafers. *J Micromech Microeng* 18(12):125021
18. Al-Halhouli AaT, Demming S, Dietzel A, Büttgenbach S (2016) Design, fabrication, and characterization of a continuous flow micropump system. *Journal of Thermal Science and Engineering Applications*, 8(2)
19. Pourmand A, Shaegh SAM, Ghavifekr HB, Najafi Aghdam E, Dokmeci MR, Khademhosseini A, Zhang YS (2018) Fabrication of whole-thermoplastic normally closed microvalve, micro check valve, and micropump. *Sensors Actuators B Chem* 262:625–636
20. Bourouina T, Grandchamp J-P (1996) Modeling micropumps with electrical equivalent networks. *J Micromech Microeng* 6(4):398
21. Gong Q, Zhou Z, Yang Y, Wang X (2000) Design, optimization and simulation on microelectromagnetic pump. *Sensors Actuators A Phys* 83(1–3):200–207
22. Khalilian S, Park SS, Freiheit T (2012) Low cost micro-pump valve design," in ASME 2012 International Design Engineering Technical Conferences and Computers and Information in Engineering Conference, pp. 151–159: American Society of Mechanical Engineers Digital Collection
23. Fournier S, Chappel E (2017) Modeling of a piezoelectric MEMS micropump dedicated to insulin delivery and experimental validation using integrated pressure sensors: application to partial occlusion management. *Journal of Sensors*, 2017
24. C. AG. (2019). Available: <https://www.tpu.covestro.com/en/Technologies/Properties/Mechanical-Properties/Stiffness>
25. Lai Z, Karney B, Yang S, Wu D, Zhang F (2017) Transient performance of a dual disc check valve during the opening period. *Ann Nucl Energy* 101:15–22
26. Nguyen N-T, Wereley ST, Shaegh SAM (2019) Fundamentals and applications of microfluidics. Artech house
27. Benra F-K, Dohmen HJ, Pei J, Schuster S, Wan B (2011) A comparison of one-way and two-way coupling methods for numerical analysis of fluid-structure interactions. *J Appl Math*, 2011
28. Shamsi A, Mazloum J (2019) Numerical study of a membrane-type micro check-valve for microfluidic applications. *Microsyst Technol*:1–10
29. Hirt C, Amsden A, Cook J (1997) An arbitrary Lagrangian–Eulerian computing method for all flow speeds. *J Comput Phys* 135(2):203–216
30. Donea J, Huerta A, Ponthot J-Ph, Rodríguez-Ferran A (2004) Arbitrary Lagrangian–Eulerian methods," in *Encyclopedia of Computational Mechanics*
31. Perdignes FA, Luque A, Quero JM (2014) Correspondence between electronics and fluids in MEMS: designing microfluidic systems using electronics. *IEEE Ind Electron Mag* 8(4):6–17
32. Wu C-H, Chen C-W, Kuo L-S, Chen P-H (2014) A novel approach to measure the hydraulic capacitance of a microfluidic membrane pump. *Adv Mater Sci Eng*, 2014
33. Shaegh SAM, Pourmand A, Nabavinia M, Avci H, Tamayol A, Mostafalu P, Ghavifekr HB, Aghdam EN, Dokmeci MR, Khademhosseini A, Zhang YS (2018) Rapid prototyping of whole-thermoplastic microfluidics with built-in microvalves using laser ablation and thermal fusion bonding. *Sensors Actuators B Chem* 255:100–109
34. Sackmann EK, Fulton AL, Beebe DJ (2014) The present and future role of microfluidics in biomedical research. *Nature* 507(7491):181
35. Guckenberger DJ, de Groot TE, Wan AM, Beebe DJ, Young EW (2015) Micromilling: a method for ultra-rapid prototyping of plastic microfluidic devices. *Lab Chip* 15(11):2364–2378
36. Korkmaz E, Onler R, Ozdoganlar OB (2017) Micromilling of poly (methyl methacrylate, PMMA) using single-crystal diamond tools. *Procedia Manufacturing* 10:683–693
37. Shaegh SAM, Wang Z, Ng SH, Wu R, Nguyen HT, Chan LCZ, Toh AGG, Wang Z (2015) Plug-and-play microvalve and micropump for rapid integration with microfluidic chips. *Microfluid Nanofluid* 19(3):557–564
38. Tsao C-W, DeVoe DL (2009) Bonding of the thermoplastic polymer microfluidics. *Microfluid Nanofluid* 6(1):1–16
39. Lian K, Ling Z-G (2002) Post-exposure heat treatment to reduce surface roughness of PMMA surfaces formed by radiation lithography, ed: Google Patents
40. Ala'aldeen T, Demming S, Dietzel A, Büttgenbach S (2016) Design, fabrication, and characterization of a continuous flow micropump system. *Journal of Thermal Science and Engineering Applications* 8(2):021006
41. G. T. Bui, J.-H. Wang, and -. L. Lin Jr, "Optimization of micropump performance utilizing a single membrane with an active check valve," *Micromachines*, vol. 9, no. 1, p. 1, 2018
42. Dumont-Fillon D, Tahriou H, Conan C, Chappel E (2014) Insulin micropump with embedded pressure sensors for failure detection and delivery of accurate monitoring. *Micromachines* 5(4):1161–1172

Publisher's Note Springer Nature remains neutral with regard to jurisdictional claims in published maps and institutional affiliations.